

SUPPLEMENTARY DATA

Supplementary Text and References

Based on the model-structure and conservation, we provide molecular-level interpretation of additional clinical mutants for which experimental data is available.

H1069Q. The most frequent mutation in Caucasian and African American population. The mutation was shown to decrease protein stability^{1,2} and cause mislocalization in mammalian cells^{2,3}. Biochemical studies determined that H1069Q substitution decreases affinity for ATP^{4,5} and markedly diminishes catalytic phosphorylation⁶. However, the transport activity is not lost entirely, since this mutant can complement yeast strain lacking endogenous copper ATPase⁷. The previous study showed that the effect of mutation on folding is likely due to inherent instability of the nucleotide-binding domain of ATP7B in the absence of ATP⁸, and the positioning of His1069 in the N-domain was resolved in an NMR study of the isolated domain⁵. In our analysis, His1069 is indeed highly conserved, and situated in the functional patch detected by PatchFinder. The model-structure provides the context of this position relative the rest of the structure, situating His1069 in the interface of the N-domain with the P-domain (Fig. S8A, Table S1). As part of the functional site, His1069 could thus be critical for interaction with ATP, with the N-terminal domains or with other proteins.

D765N. Asp765 is highly conserved, located in the model at the extracellular end of TM4. Equivalent to LCopA Glu189, Asp765 probably is important for the copper exit site as well, as suggested by Gourdon et al. for LCopA⁹. This ascribes Asp765 a role in the copper transport mechanism, and suggests that the negative charge can only be partly compensated by

the Asn polar side-chain (Fig. 5D, Table S1). The study of Huster et al. supported this role, revealing partial transport activity of the D765N mutant as well as decreased expression¹⁰.

G710S and G712D of the mouse ATP7B, matching human Gly711. The G710S mutant was recently characterized, exhibiting complete loss of activity in copper uptake¹⁰. The mouse equivalent to Gly711, Gly712, was also examined upon mutation to Asp. The mutation is associated with copper accumulation in the liver and liver disease as well as slight increase of copper in the brain¹¹. Our analysis suggested a deleterious effect to a substitution in Gly711, since it is highly conserved, while we could not determine the sensitivity to mutation of mediocly conserved Gly710 based on accessibility and conservation alone. Further examining the structural location of these positions, we observed that the model places Gly710 and Gly711 in the kinked region in TM2, strongly suggests a role in conformational changes during transport cycle (Fig. S8B, Table S1).

REFERENCES

1. P. V. van den Berghe, J. M. Stapelbroek, E. Krieger, P. de Bie, S. F. van de Graaf, R. E. de Groot, E. van Beurden, E. Spijker, R. H. Houwen, R. Berger, L. W. Klomp, Reduced expression of ATP7B affected by Wilson disease-causing mutations is rescued by pharmacological folding chaperones 4-phenylbutyrate and curcumin. *Hepatology* 2009, *50*. 1783-95.
2. A. S. Payne, E. J. Kelly, J. D. Gitlin, Functional expression of the Wilson disease protein reveals mislocalization and impaired copper-dependent trafficking of the common H1069Q mutation. *Proc Natl Acad Sci U S A* 1998, *95*. 10854-9.
3. D. Huster, M. Hoppert, S. Lutsenko, J. Zinke, C. Lehmann, J. Mossner, F. Berr, K. Caca, Defective cellular localization of mutant ATP7B in Wilson's disease patients and hepatoma cell lines. *Gastroenterology* 2003, *124*. 335-45.
4. C. T. Morgan, R. Tsivkovskii, Y. A. Kosinsky, R. G. Efremov, S. Lutsenko, The distinct functional properties of the nucleotide-binding domain of ATP7B, the human copper-transporting ATPase: analysis of the Wilson disease mutations E1064A, H1069Q, R1151H, and C1104F. *J Biol Chem* 2004, *279*. 36363-71.
5. O. Dmitriev, R. Tsivkovskii, F. Abildgaard, C. T. Morgan, J. L. Markley, S. Lutsenko, Solution structure of the N-domain of Wilson disease protein: distinct nucleotide-binding environment and effects of disease mutations. *Proc Natl Acad Sci U S A* 2006, *103*. 5302-7.
6. R. Tsivkovskii, R. G. Efremov, S. Lutsenko, The role of the invariant His-1069 in folding and function of the Wilson's disease protein, the human copper-transporting ATPase ATP7B. *J Biol Chem* 2003, *278*. 13302-8.

7. M. Iida, K. Terada, Y. Sambongi, T. Wakabayashi, N. Miura, K. Koyama, M. Futai, T. Sugiyama, Analysis of functional domains of Wilson disease protein (ATP7B) in *Saccharomyces cerevisiae*. *FEBS Lett* 1998, *428*. 281-5.
8. O. Y. Dmitriev, A. Bhattacharjee, S. Nokhrin, E. M. Uhlemann, S. Lutsenko, Difference in stability of the N-domain underlies distinct intracellular properties of the E1064A and H1069Q mutants of copper-transporting ATPase ATP7B. *J Biol Chem* 2011, *286*. 16355-62.
9. P. Gourdon, X. Y. Liu, T. Skjorringe, J. P. Morth, L. B. Moller, B. P. Pedersen, P. Nissen, Crystal structure of a copper-transporting PIB-type ATPase. *Nature* 2011, *475*. 59-64.
10. K. A. Huster D, Bhattacharjee A, Raines L, Jantsch V, Noe J, Schirrmeister W, Sommerer I, Sabri O, Berr F, Mossner J, Stieger B, Caca K, Lutsenko S, Diverse Functional Properties of Wilson Disease ATP7B Variants. *Gastroenterology* 2011, *in press*.
11. V. Coronado, M. Nanji, D. W. Cox, The Jackson toxic milk mouse as a model for copper loading. *Mammalian Genome* 2001, *12*. 793-795.
12. M. Kalman, N. Ben-Tal, Quality assessment of protein model-structures using evolutionary conservation. *Bioinformatics* 2010, *26*. 1299-307.
13. J. D. Thompson, T. J. Gibson, D. G. Higgins, Multiple sequence alignment using ClustalW and ClustalX. *Curr Protoc Bioinformatics* 2002, *Chapter 2*. Unit 2 3.
14. S. M. Kenney, D. W. Cox, Sequence variation database for the Wilson disease copper transporter, ATP7B. *Hum Mutat* 2007, *28*. 1171-7.
15. H. Ashkenazy, E. Erez, E. Martz, T. Pupko, N. Ben-Tal, ConSurf 2010: calculating evolutionary conservation in sequence and structure of proteins and nucleic acids. *Nucleic Acids Res* 2010, *38*. W529-33.
16. A. Gupta, A. Bhattacharjee, O. Y. Dmitriev, S. Nokhrin, L. Braiterman, A. L. Hubbard, S. Lutsenko, Cellular copper levels determine the phenotype of the Arg875 variant of ATP7B/Wilson disease protein. *Proc Natl Acad Sci USA* 2011, *108*. 5390-5.
17. S. Park, J. Park, G. H. Kim, J. H. Choi, K. M. Kim, J. B. Kim, H. W. Yoo, Identification of novel ATP7B gene mutations and their functional roles in Korean patients with Wilson disease. *Human Mutation* 2007, *28*. 1108-1113.
18. J. R. Forbes, D. W. Cox, Functional characterization of missense mutations in ATP7B: Wilson disease mutation or normal variant? *Am J Hum Genet* 1998, *63*. 1663-74.
19. G. Hsi, L. M. Cullen, G. Macintyre, M. M. Chen, D. M. Glerum, D. W. Cox, Sequence variation in the ATP-binding domain of the Wilson disease transporter, ATP7B, affects copper transport in a yeast model system. *Hum Mutat* 2008, *29*. 491-501.
20. M. B. Theophilos, D. W. Cox, J. F. B. Mercer, The Toxic Milk Mouse is a Murine Model of Wilson Disease. *Human Molecular Genetics* 1996, *5*. 1619-1624.
21. I. Voskoboinik, M. Greenough, S. La Fontaine, J. F. Mercer, J. Camakaris, Functional studies on the Wilson copper P-type ATPase and toxic milk mouse mutant. *Biochem Biophys Res Commun* 2001, *281*. 966-70.

SUPPLEMENTARY FIGURES

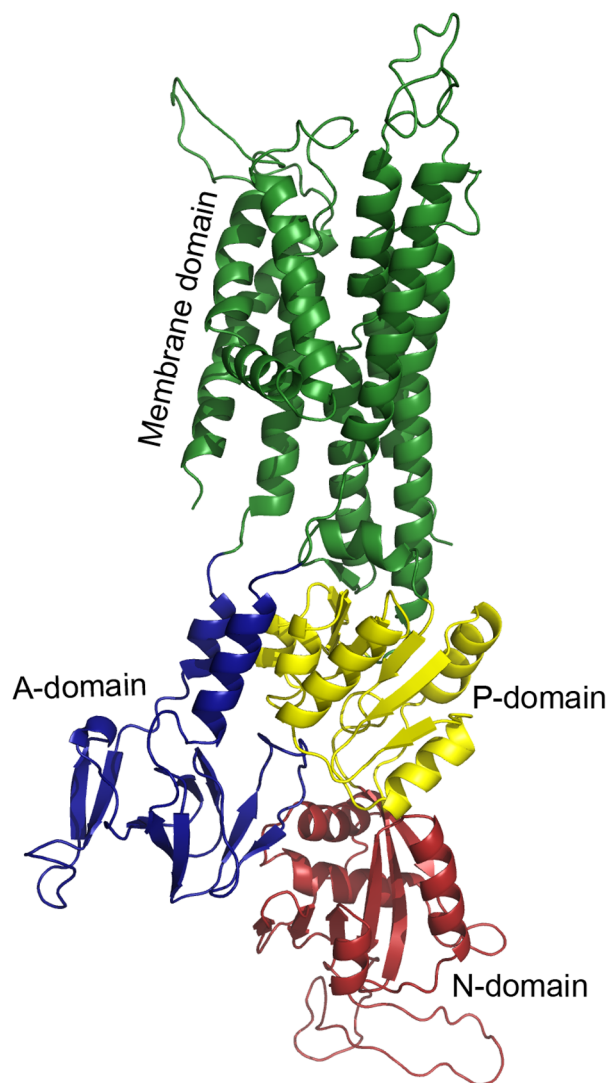


Figure S1. Overall architecture of the ATP7B model-structure. The ATP7B model, consisting of positions 643-1377 of the 1465 amino acid sequence, is shown as cartoon and viewed from the side, with the cytoplasm below. The membrane helices, and the A-, N- and P-domains are colored green, blue, red and yellow, respectively.

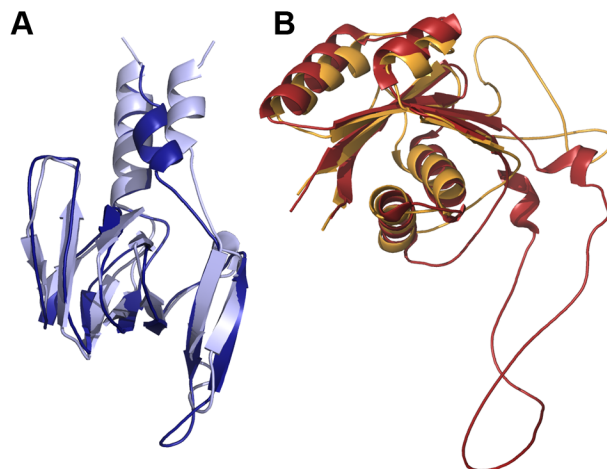


Figure S2. Comparison to NMR data. **A.** The NMR structure of the A-domain from ATP7A (PDB ID 2KIJ, light blue) was aligned to the corresponding domain from the ATP7B model (dark blue) using PyMol (<http://www.pymol.org/>) **B.** The NMR structure of the unbound form of the N-domain, solved for ATP7A (PDB ID 2KMV, orange) aligned to the N-domain in the ATP7B model (red). Excluding the flexible loop regions, it is apparent that both NMR structures show excellent agreement with the domains conformation from the model of the entire core structure.

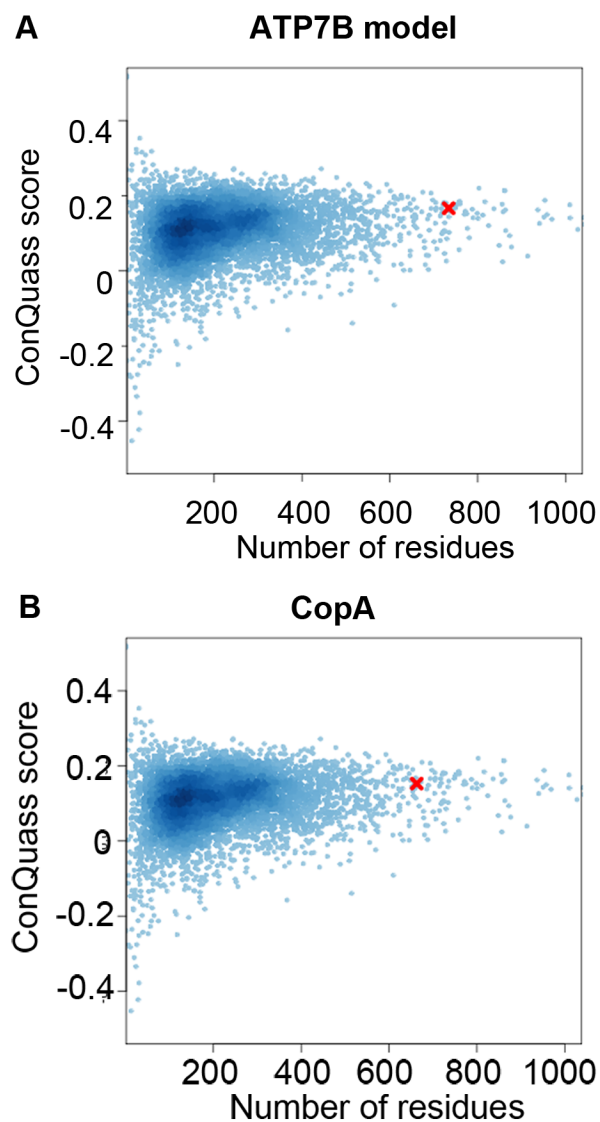


Figure S3. ConQuass scores¹² of the ATP7B model and LCopA structure. In both panels, the ConQuass scores of all the structures in the Protein Data Bank (PDB) are shown as blue dots, and displayed as a function of the number of residues in the structures. The ConQuass scores of the ATP7B model (panel A) and LCopA structure⁹ (panel B) are marked in red. It is evident that both receive high probability scores, with that of ATP7B model slightly exceeding that of the LCopA crystal structure.

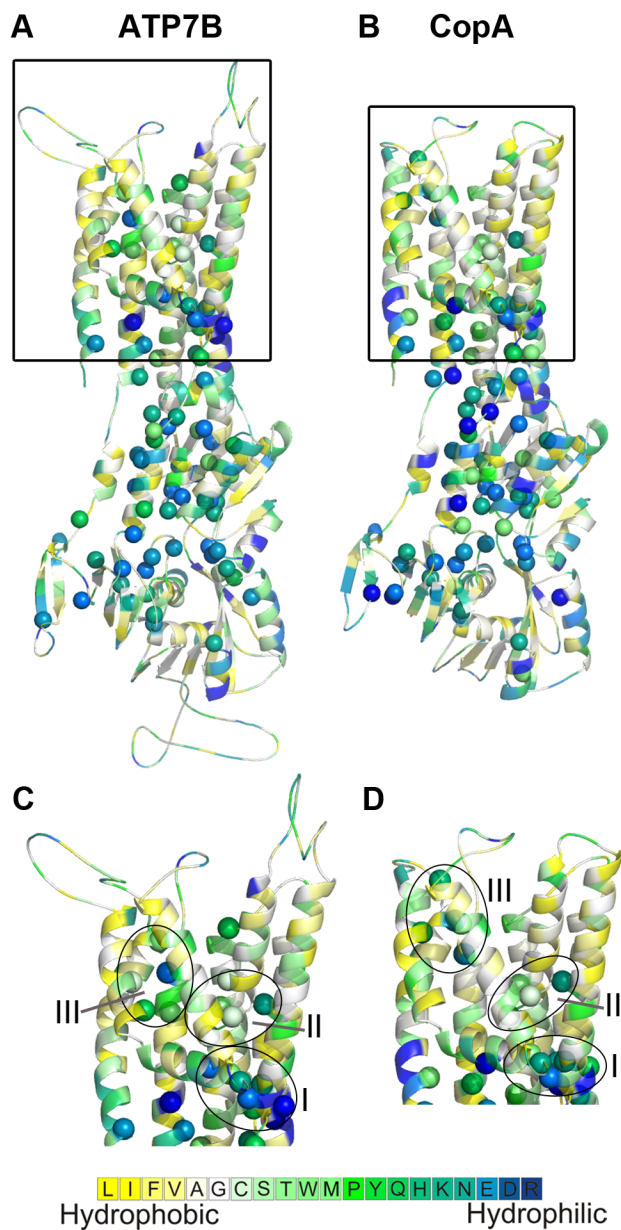


Figure S4. Hydrophobicity analysis of ATP7B and LCopA- three highly conserved and hydrophilic sites in the membrane domain. In panels **A** and **B**, the ATP7B model and LCopA structure are displayed in cartoon representation, and displayed from the side with the cytoplasm below. C α atoms of highly hydrophilic positions, as well as of potential Cu⁺ binding Met and Cys, which are also highly conserved (with ConSurf grades of 7-9), are shown as spheres. Panels **C** (ATP7B) and **D** (LCopA) show a zoom-in of the membrane domains, emphasized in squares in the matching panels **A** and **B**. The three membrane regions containing highly conserved polar residues are marked with squares and numbered. Roman letters I, II and III correspond to the potential entry, membrane site and exit, respectively.

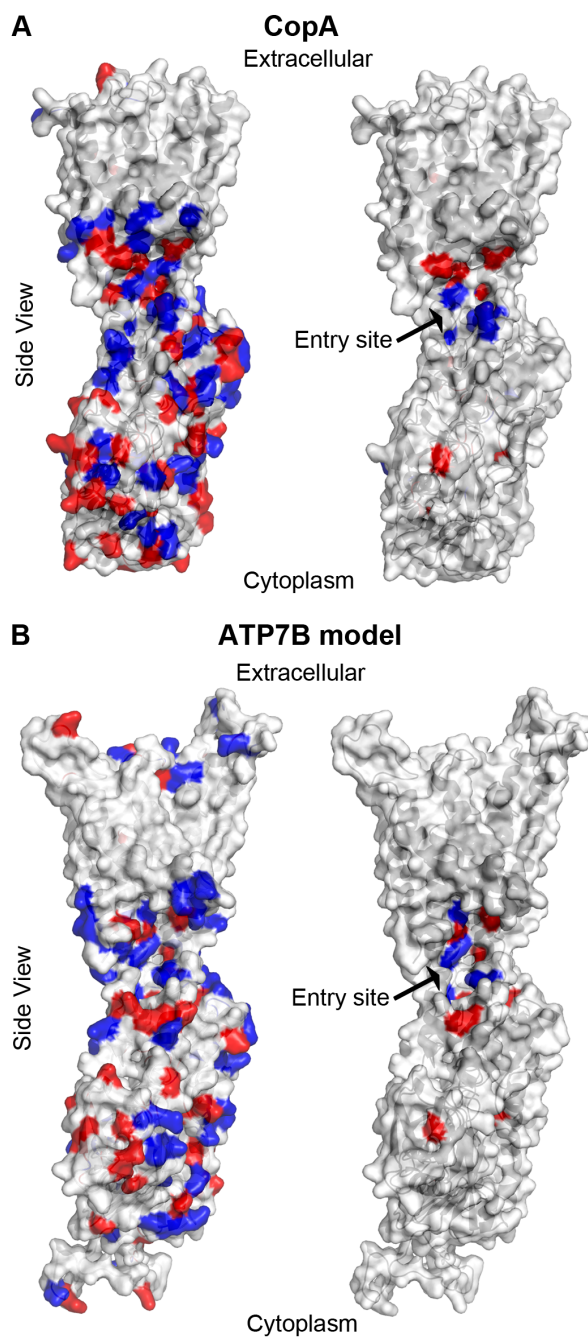


Figure S5. Mapping of charged residues on the LCopA structure and ATP7B model. Side view of the LCop structure (A) and ATP7B model (B), colored white and shown in partly transparent surface representation. On the structures shown on left hand side, all the negatively and positively charged residues are colored red and blue, respectively. On the right hand side, only charged residues that are highly conserved (ConSurf grades of 8 and 9) are colored. It is apparent that most of the charged residues are not highly conserved, and are mapped to the cytoplasmic domains. A single cluster of highly conserved residues is evident in both structures, which is mapped to the copper membrane entry site (marked).

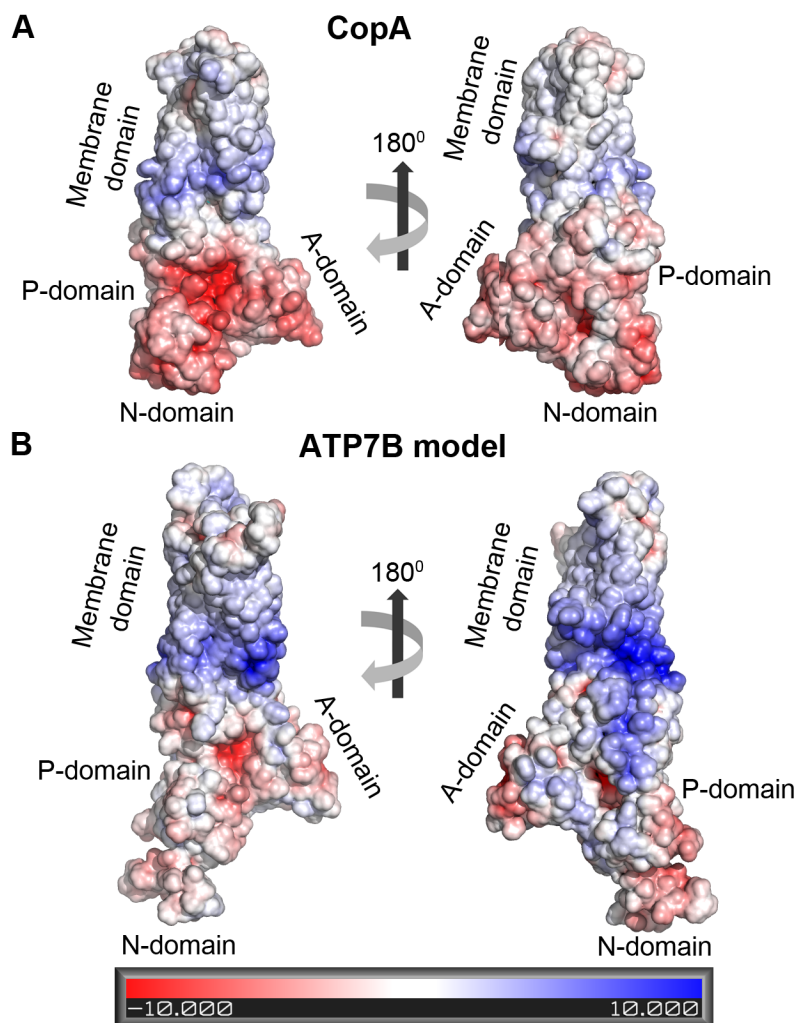


Figure S6. Mapping of electrostatic potential on the surface LCopA structure and ATP7B model. Two-side view of the LCop structure (A) and ATP7B model (B) with the cytoplasm below. The structures are shown in surface representation and colored by electrostatic potential according to the legend below, as computed by solving the non-linearized version of the Adaptive Poisson Boltzman Solver (APBS) software (reference below). It is apparent that both structures contain a negatively charged patch at the interface between the soluble domains (left hand side), which is more emphasized at the LcopA structure. The ATP7B model, on the other hand, shows a more prominent positively charged region, situated around the presumed membrane boundaries at the cytoplasmic side.

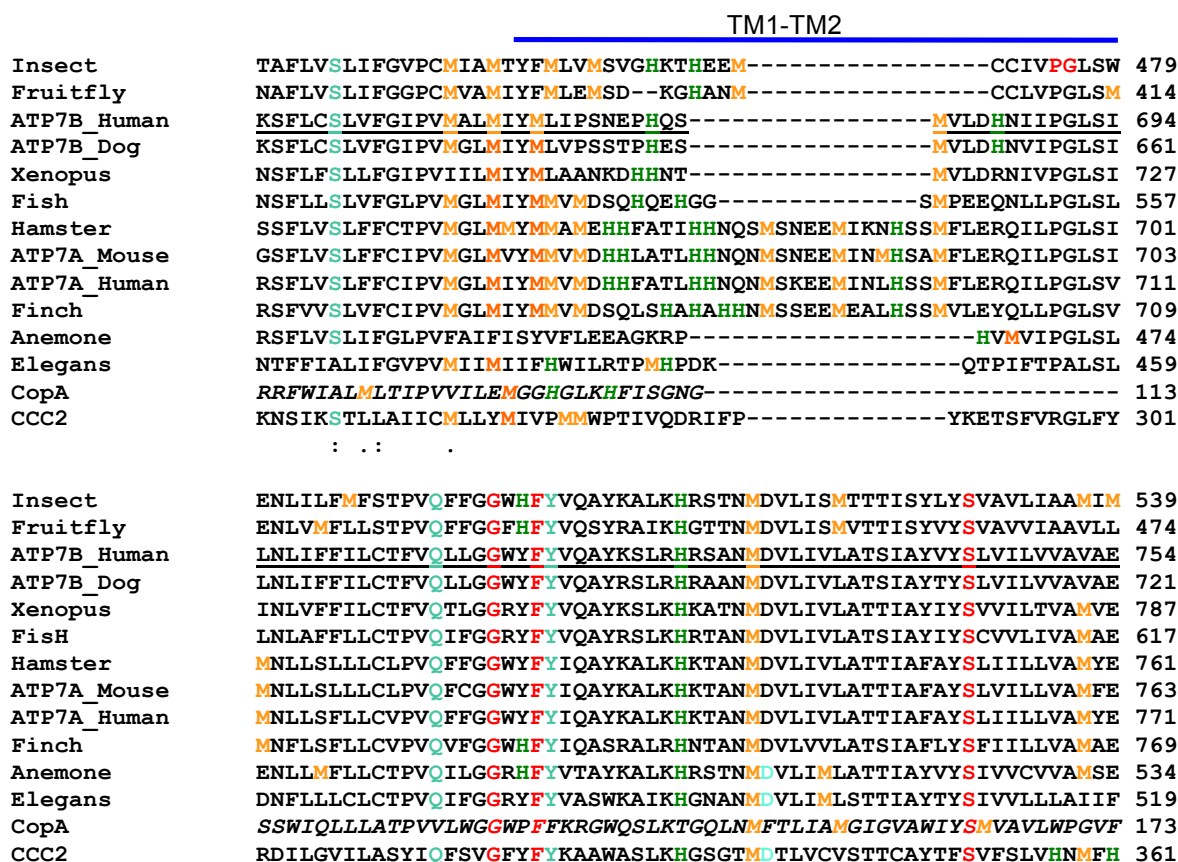


Figure S7. Sequence alignment of eukaryotic Cu-ATPases in the region of TM1-TM2 transmembrane segment. Sequences were aligned using ClustalW¹³. Conserved positions and copper preferred ligators His, Met and Cys, are highlighted in colors. The TM1-TM2 loop is marked by a blue line. ATP7B sequence is underlined; and bacterial sequence (CopA) is in italic. It is apparent that TM1,2 loop is longer in eukaryotic pumps and that the entire TM1,2 region is more hydrophilic and enriched in Met and His residues

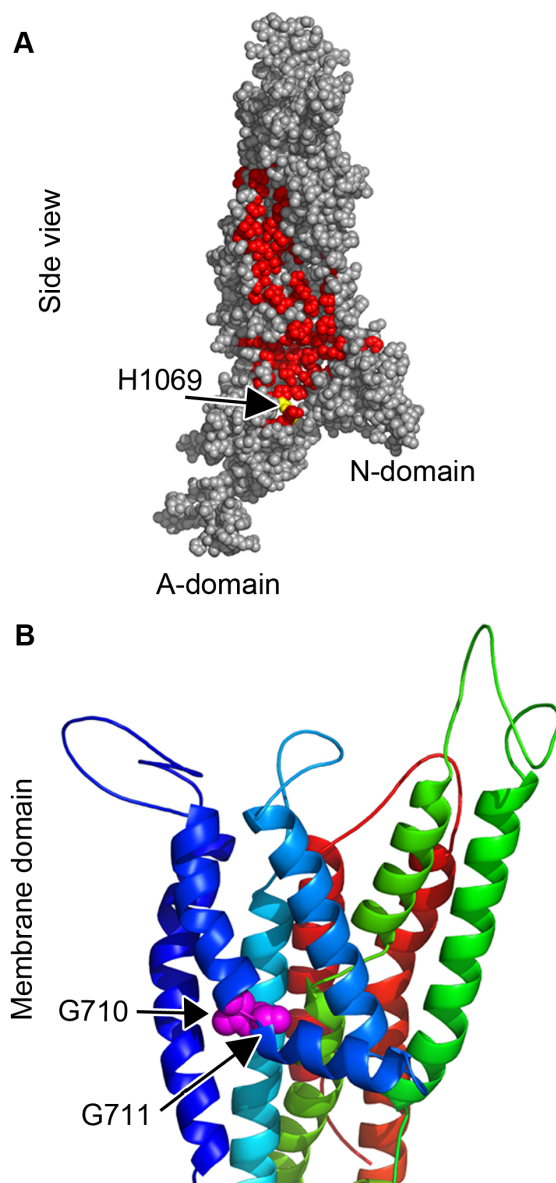


Figure S8. Structural interpretation of His1069, Gly710 and Gly711. Side view of the ATP7B model with the cytoplasm below. **A.** The model is shown as gray spheres with the PatchFinder functional site in red. His1069, colored yellow and marked, is situated on the A-domain, interfacing the N-domain, and is part of the predicted functional site. **B.** Zoom into the membrane domain, with model colored by rainbow. Gly710 and Gly711 (magenta) are situated at the kinked segment of TM2, thus can contribute to the flexibility and conformation of the helix.

Table S1. Clinical mutations evaluated experimentally. The columns show the position, clinical substitutions ¹⁴, ConSurf conservation grade (¹⁵, with 1-9 indicating variable-to-conserved), relative solvent accessibility inclusion in the PatchFinder functional site and experimental results, from left to right. In addition, the suggested sensitivity was ascribed using an approach based on conservation and accessibility. Positions proposed as sensitive if conserved (grades 8 or 9) and buried (SASA <10%), or part of the functional PatchFinder site. On the other hand, variable (grades 1-2) and exposed (SASA >10%) positions were suggested as not sensitive to mutation. For all other positions, not falling under these distinct categories, the sensitivity of the position was not suggested. Green shade marks suggestions that agreed with the experimental result, red marks the suggestion that contradicted the experiments, whereas yellow mark positions for which we could not suggest the position's sensitivity. We excluded from this analysis positions such as Lys832, for which the experimental effect of mutation was only partial (<50% decreased activity), as such experiments cannot clearly indicate whether the positions in question are indeed sensitive or non-sensitive to substitutions.

Position	Mut.	Co n.	SAS A (%)	Patch-Finder	Location	Exp. effect	Suggested sensitivity	Ref.
M645	R	1	98.4	NO	TM1	Normal copper transport	Not sensitive	10
G710	R, S, A, V	5	0	NO	TM2	Low copper transport	-	10
G711	R, W, E	9	7.8	NO	TM2	Copper accumulation in the liver, liver disease, slight increase in the brain	Sensitive	11
P760	L	4	5.2	NO	Loop 3-4	Low copper transport	-	10
D765	N, G	8	3.9	NO	TM4	Low transport activity, decreased expression	Sensitive	10
R778	G, W, Q, L	8	17.8	NO	TM4	Lower stability and abnormal localization	-	1, 2
P840	L	9	8.3	NO	A-domain	Very low copper transport	Sensitive	10
I857	T	7	17.6	NO	A-domain	Decreased transport but does not significantly inhibit catalytic dephosphorylation.	-	10
A874	V	8	11.5	NO	A-domain	Misfolded and mistargeted (located in the ER), no activity	-	¹⁰ and current study
G875	R	8	17.2	NO	A-domain	Destabilizes the A-domain, decreases affinity for ATP,	-	16

						normal transport and trafficking		
I929	V	6	58.2	NO	TM5	Full complementation in yeast	-	17
G943	S, C, D	6	18.2	NO	TM5	Affects folding	-	1, 4, 18
P992	L, H	9	8.3	NO	TM6	Inactivation in yeast complementation assay, affects folding, Very low copper transport	Sensitive	1, 4, 18, 10
V995	A	9	15.9	NO	TM6	Normal variant (based on studies in yeast)	-	18
D1027	A	9	6.3	YES	P-domain	No copper transport	Sensitive	10
T1031	S, A	9	6	NO	P-domain	Significantly decreased but measurable transport activity	Sensitive	10
R1041	W, P	6	67.5	NO	N-domain	Full complementation in yeast	-	19
P1052	L	2	59.1	NO	P-domain	Very low copper uptake	Not sensitive	10
E1064	K, A	9	10.1	YES	N-domain	Inactivation in yeast complementation assay, No copper transport	Sensitive	4, 8, 10, 19
H1069	Q	9	30.2	YES	N-domain	Decrease protein stability and cause mislocalization in mammalian cells. Decreases affinity for ATP and markedly diminished catalytic phosphorylation, Low copper transport	Sensitive	1-6, 10
C1104	F, Y	6	5.9	NO	N-domain	Affects folding	-	1, 4, 18
V1106	I, D	6	3.3	NO	N-domain	Inactivation in yeast complementation assay	-	19
A1140	V	1	35.7	NO	N-domain	Full complementation in yeast	Not sensitive	19
R1151	C, H	2	74.3	NO	N-domain	Small effect on folding of the N-domain	Not sensitive	4
A1183	T, G	7	0	NO	N-domain	Full complementation in yeast	-	19
G1186	S, C	2	75.7	NO	N-domain	Full complementation in yeast	Not sensitive	19

G1213	V	8	93.3	NO	P-domain	Complete loss of transport	-	10
D1222	N,Y,V	9	35.4	YES	P-domain	D1222V- Very low copper transport	Sensitive	10
V1262	F	9	1.1	NO	P-domain	Affects folding	Sensitive	1, 4, 18
G1266	R,K,V	9	0	NO	P-domain	G1266R- Very low copper uptake	Sensitive	10
N1270	T, S	9	1.9	YES	P-domain	Inactivation in yeast complementation, Low copper uptake	Sensitive	7, 10
P1273	S,L,Q	9	0	NO	TM8	Very low copper uptake	Sensitive	10
M1359	I	9	16.5	YES	TM8	Copper accumulation and liver disease in mice, lacked a measurable transport activity in copper uptake assay	Sensitive	20, 21
S1363	F	9	29.4	YES	TM8	Affects folding	Sensitive	1, 4, 18

Table S2. Suggested sensitivity to mutation. The 197 positions in which clinical mutations were detected¹⁴ [ENREF 14](#) and are included in the ATP7B model-structure. The detected substitution, ConSurf evolutionary conservation (grades 1-9 for variable-to-conserved) and relative surface accessibility are shown under Mut., Con., and SASA, respectively. The PatchFinder column indicates whether the position was detected as a part of the functional site derived from this analysis. Last, the suggested sensitivity is based on the criteria described in the main text and in Table S1, incorporating conservation and accessibility to suggest the outcome of mutation only for positions for concurring with our criteria.

Position	Mut.	Con.	SASA (%)	PatchFinder	Suggested sensitivity
L1043	P	1	9.8	NO	-
G1089	E,V	1	19.2	NO	Not sensitive
A1168	S,P	1	22.8	NO	Not sensitive
A1140	V	1	35.7	NO	Not sensitive
G1111	D	1	62.6	NO	Not sensitive
N676	I	1	65.1	NO	Not sensitive
R1228	T	1	68.2	NO	Not sensitive
H1207	R	1	72.5	NO	Not sensitive
Q1142	H	1	79.6	NO	Not sensitive
K952	R	1	87.2	NO	Not sensitive
M645	R	1	98.4	NO	Not sensitive
V949	G	1	107	NO	Not sensitive
D1047	V	1	119.9	NO	Not sensitive
I1184	T	2	6.7	NO	-
T1143	N	2	34	NO	Not sensitive
A756	G,V	2	45.7	NO	Not sensitive
L1305	P	2	46.7	NO	Not sensitive
R1156	H	2	48.8	NO	Not sensitive
T933	P	2	57.2	NO	Not sensitive
P1052	L	2	59.1	NO	Not sensitive
R919	G,W	2	60.1	NO	Not sensitive
A1065	P	2	63.3	NO	Not sensitive
D1164	N	2	67.7	NO	Not sensitive
R1038	K	2	69.1	NO	Not sensitive
Q1095	P	2	69.9	NO	Not sensitive
R1151	C,H	2	74.3	NO	Not sensitive
R758	M	2	75.2	NO	Not sensitive
D1215	Y	2	75.7	NO	Not sensitive
G1186	S,C	2	75.7	NO	Not sensitive
C1375	S	2	80.4	NO	Not sensitive
T1232	P	2	85.3	NO	Not sensitive

Q1200	P	2	106.7	NO	Not sensitive
K832	R	3	39.5	NO	-
C1091	Y	3	74.3	NO	-
P690	L	3	85.9	NO	-
P760	L	4	5.2	NO	-
M1169	V,T	4	14.9	NO	-
R969	W,Q	4	25	NO	-
I967	F	4	36.8	NO	-
V1109	M	4	38.1	NO	-
L708	P	4	55.3	NO	-
P1098	R	4	55.8	NO	-
V1036	I	4	68.2	NO	-
L1368	P	4	70.1	NO	-
V1334	D	4	74.5	NO	-
R827	P	4	85.2	NO	-
G710	R,S,A,V	5	0	NO	-
I747	F	5	0.7	NO	-
V1146	M	5	3.1	NO	-
Y713	C	5	42.1	NO	-
M665	I	5	60.4	NO	-
S693	P,C,Y	5	63.7	NO	-
L1083	F	5	78.9	NO	-
T974	M	6	2.7	NO	-
I1148	T	6	2.9	NO	-
V1106	I,D	6	3.3	NO	-
W1153	R,C	6	5.4	NO	-
C1104	F,Y	6	5.9	NO	-
S653	Y	6	8	NO	-
Y741	C	6	10.8	NO	-
A1063	V	6	13.9	NO	-
G943	S,C,D	6	18.2	NO	-
S975	Y	6	21.3	NO	-
G691	R	6	38	NO	-
I929	V	6	58.2	NO	-
R1041	W,P	6	67.5	NO	-
Q1004	P	6	80.6	NO	-
A1183	T,G	7	0	NO	-
C703	Y	7	0	NO	-
M1025	R	7	0.1	NO	-
V1252	I	7	0.7	NO	-
S721	P	7	2.2	NO	-

A1193	P	7	2.4	NO	-
P768	H,L	7	2.5	NO	-
V1024	A	7	4.4	NO	-
V1297	I,D	7	4.9	NO	-
A1018	V	7	5.8	NO	-
I1102	T	7	10.7	NO	-
I857	T	7	17.6	NO	-
Y715	H	7	20.3	NO	-
L1255	I	7	23.2	NO	-
M769	V,R,I,L	7	29.4	NO	-
L776	P,V	7	31.5	NO	-
T888	P	7	34.4	NO	-
E1173	K,G	7	43.3	NO	-
R1322	P	7	53	NO	-
W1353	R	7	79.3	NO	-
G869	V,R	7	134.4	NO	-
G1341	S,R,D,V	8	0	NO	Sensitive
G1061	E	8	0.4	NO	Sensitive
A971	V	8	1.1	NO	Sensitive
F763	Y	8	3.5	NO	Sensitive
T977	M	8	3.7	NO	Sensitive
D765	N,G	8	3.9	NO	Sensitive
V1216	M	8	4.2	NO	Sensitive
G1176	R,E	8	4.5	NO	Sensitive
R1320	S	8	5.2	NO	Sensitive
S921	N	8	5.3	NO	Sensitive
S657	R	8	5.4	NO	Sensitive
T935	M	8	8.4	NO	Sensitive
V825	L	8	9.9	NO	Sensitive
L979	Q	8	10.3	NO	-
T766	P,M,R	8	10.3	NO	-
A874	V	8	11.5	NO	-
I1230	V	8	13.8	NO	-
G875	R	8	17.2	NO	-
R778	G,W,Q,L	8	17.8	NO	-
D1279	Y,G	8	21.2	NO	-
V890	M	8	22.9	NO	-
L1327	V	8	23.5	NO	-
D1296	N	8	24.5	NO	-
V1239	G	8	26.1	NO	-
A727	V,D	8	26.7	NO	-

G1012	R,V	8	30.8	NO	-
Q1256	R	8	36.1	NO	-
V864	I	8	50.5	NO	-
Q898	R	8	63.5	NO	-
F1094	L	8	71.6	NO	-
G1213	V	8	93.3	NO	-
D1271	N,E	9	0	NO	Sensitive
G1266	R,K,V	9	0	NO	Sensitive
G843	R	9	0	NO	Sensitive
G998	D	9	0	NO	Sensitive
P1273	S,L,Q	9	0	NO	Sensitive
S744	P	9	0	NO	Sensitive
A1328	T	9	0.2	NO	Sensitive
C985	Y	9	0.2	NO	Sensitive
G1281	C,D	9	0.4	YES	Sensitive
I1336	T	9	0.4	NO	Sensitive
A982	V	9	0.6	NO	Sensitive
K1248	N	9	0.9	NO	Sensitive
T1220	M	9	0.9	NO	Sensitive
A1241	V	9	1	YES	Sensitive
V1262	F	9	1.1	NO	Sensitive
A1278	V	9	1.2	YES	Sensitive
T1033	A,S	9	1.3	YES	Sensitive
N1270	T,S	9	1.9	YES	Sensitive
I1236	T	9	2.9	NO	Sensitive
D842	N	9	3.2	YES	Sensitive
C980	Y	9	4	NO	Sensitive
L1373	P,R	9	4.4	YES	Sensitive
A803	T	9	4.6	NO	Sensitive
G1221	E	9	4.8	YES	Sensitive
G1149	A	9	5.3	NO	Sensitive
T737	R	9	5.5	NO	Sensitive
L1299	F	9	5.6	NO	Sensitive
T1031	S,A	9	6	NO	Sensitive
N878	K	9	6.1	NO	Sensitive
D1027	A	9	6.3	YES	Sensitive
N1332	D,K	9	6.7	NO	Sensitive
P1245	S,T	9	6.8	YES	Sensitive
G711	R,W,E	9	7.8	NO	Sensitive
P840	L	9	8.3	NO	Sensitive
P992	L,H	9	8.3	NO	Sensitive

G988	R,V	9	8.6	NO	Sensitive
W939	C	9	9.9	NO	Sensitive
I899	F	9	10	YES	Sensitive
E1064	K,A	9	10.1	YES	Sensitive
T1029	A,I	9	10.3	YES	Sensitive
M729	V	9	11.6	YES	Sensitive
A1358	S	9	12.1	YES	Sensitive
S1310	R	9	12.1	NO	-
V731	E	9	12.3	NO	-
S876	F	9	13.1	YES	Sensitive
V1243	M	9	14.5	NO	-
D1267	A,V	9	14.6	YES	Sensitive
T991	M,T	9	15	NO	-
S1369	L	9	15.3	YES	Sensitive
T993	M	9	15.3	YES	Sensitive
V995	A	9	15.9	NO	-
M1359	I	9	16.5	YES	Sensitive
N728	D	9	18	YES	Sensitive
G1355	S	9	21.4	NO	-
P1352	S,L,R	9	21.5	NO	-
T858	A	9	23.5	YES	Sensitive
S1363	F	9	29.4	YES	Sensitive
H1069	Q	9	30.2	YES	Sensitive
D1222	N,Y,V	9	35.4	YES	Sensitive
G1268	R	9	36	YES	Sensitive
M996	T	9	37.9	YES	Sensitive
G1101	R	9	41.1	NO	-
D918	N,A,E	9	41.3	YES	Sensitive
Y1331	S	9	41.6	YES	Sensitive
A1003	T,V	9	46.7	YES	Sensitive
A861	T	9	48.1	YES	Sensitive
K1010	R,T	9	53.9	YES	Sensitive
L795	F,R	9	55.1	YES	Sensitive
T1178	A	9	60.4	NO	-
L1371	P	9	71.1	YES	Sensitive
T1288	R,M	9	73	YES	Sensitive
G1035	V	9	74.3	YES	Sensitive
G1099	S	9	85.6	NO	-
G1000	R	9	90	YES	Sensitive
T788	I	9	94.9	YES	Sensitive
E1068	G	9	100	YES	Sensitive

G891	D,V	9	100.8	YES	Sensitive
G1287	S	9	104.6	YES	Sensitive